Vol 14 No 12, December 2005
1009-1963/2005/14(12)/2522-07
Chinese Physics
© 2005 Chin. Phys. Soc.
and IOP Publishing Ltd

Local resonant characteristics of a layered cylinder embedded in the elastic medium*

Qin Bo(秦 波), Chen Jiu-Jiu(陈久久), and Cheng Jian-Chun(程建春)†

State Key Laboratory of Modern Acoustic and Institute of Acoustics, Nanjing University, Nanjing 210093, China

(Received 2 February 2005; revised manuscript received 27 June 2005)

Three kinds of resonant modes of a single layered circular elastic cylinder embedded in the elastic medium are analysed by considering the oscillation of the scatter's core, based on the fact that the core moves as a rigid body when the shell material is very compliant. The resonant frequencies of the single resonator acquired by our method are in good agreement with those calculated by the local interaction simulation approach (LISA) for the local resonant phononic crystal. Therefore, the local resonant characteristics of a single layered circular elastic cylinder can be used to evaluate the resonant frequencies of the phononic crystal. The effects of the geometrical and physical parameters of the shell and the core are also studied in details. This work is significant for designing the locally resonant phononic crystal based on the local resonant characteristics of the single resonator, and the resonant frequencies can be tuned by selecting the geometrical sizes and the materials.

Keywords: elastic wave, local resonance, layered cylinder
PACC: 4320, 6265

1. Introduction

In the last few years, the existence of forbidden gaps in band structures of acoustic and elastic wave propagations in periodic composite materials has received a great deal of attention.[1−6] Acoustic gaps are frequency domains in which propagations of sound and elastic waves are forbidden. The designing of forbidden gaps in transmission spectra has been a subject of great interest, which may have many engineering applications. Recently, the idea of local resonance for a layered spherical crystal structure has been proposed by Liu *et al.*[7] A new band gap identified in a frequency range that is significantly lower than that of an ordinary crystal structure could be predicted because of local resonance, for which the acoustic energy is absorbed by the resonance happening in a spherical core and its coating. To a certain extent, the characteristics of band gap for a locally resonant phononic crystal are determined by the resonant characteristics of a single resonator. The multiple-scattering theory method,[8−10] the finite element method,[11,12] and the local interaction simulation approach (LISA)[13] have been employed to calculate the band gap of phononic crystal which consists of multiple resonators, but all of them are very complicated.

As a micromechanics model for composites, the resonance of a single layered scatter often serves as the basis of analysing the band gap (or the strong attenuation bands) of the locally resonant phononic crystals. Much work has been done on the study of wave scattering from a single cylindrical object embedded in elastic media since 1950.[14−19] A single layered cylinder subjected to a plane-strain wave has been studied in recent years.[20−23] Numerical results confirm the existence of a resonant mode when the shell material is very compliant.[23] The resonant frequencies of phonic crystal which consists of layered circular elastic cylinders have been studied by LISA simulation.[13] Because LISA simulations for low frequencies are very computer time consuming (the time discretization step must be sufficiently small in order to guarantee the numerical stability of the algorithm) and the exact analytical solution of the problem is impossible, it is desirable to find a simple method to evaluate the resonant frequencies of the local resonant

*Project supported by the Funds for outstanding Youth Researchers from the National Natural Science Foundation of China (Grant No 10125417) and the State Key Development Program for Basic Research of China (Grant No 51307).
†E-mail: jccheng@nju.edu.cn

phononic crystal.

In this paper, the resonant frequencies and three kinds of typical resonant modes of a single layered circular cylinder for an incident longitudinal plane are analysed by considering the oscillation of the scatter's core, based on the fact that the core moves as a rigid body when the shell material is very compliant. The resonant frequencies of the single layered circular cylinder, acquired by our method are in good agreement with those calculated by the LISA simulation[13] for a locally resonant phononic crystal. Thus the resonant characteristics of the phononic crystal, which consists of layered cylinders, can be evaluated by the local resonant characteristics of the single layered cylinder. The effects of the geometrical and physical parameters of the layered cylinder are studied in details.

2. Formulation and solution of the problem

Let us assume a longitudinal plane wave incident normally on an interphase between the matrix and the layered cylinder. The single layered cylinder consists of a shell and a core as shown in Fig.1. In order to obtain the wave field of all three materials, we use the standard normal-mode expansion procedure to describe the solution in a cylindrical coordinate system. The unit scalar potential φ for the incident longitudinal plane wave can be written as

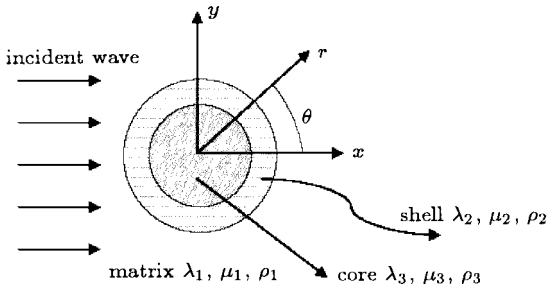


Fig.1. Geometry of the elastic wave scattering from a layered cylinder system.

$$\varphi_{\rm inc}^{(1)} = \exp(-{\rm i}\omega t)\exp({\rm i}k_{l1}r\cos\theta), \tag{1}$$

where θ and r are the polar angle and radius, respectively, k_{l1} the wave number of the longitudinal wave in the matrix material, and ω the angular frequency. After the expanding of $\exp({\rm i}k_{l1}r\cos\theta)$ in series, the incident longitudinal wave $\varphi_{\rm inc}^{(1)}$ can be expressed in the form

$$\varphi_{\rm inc}^{(1)} = \sum_{n=0}^{\infty} \varepsilon_n {\rm i}^n J_n(k_{l1}r)\cos n\theta, \tag{2}$$

where $\varepsilon_n = 2$ for $n > 0$ and $\varepsilon_n = 1$ for $n = 0$, $J_n(\cdot)$ are the nth-order Bessel functions of the first kind. The time-dependent term $\exp(-{\rm i}\omega t)$ is suppressed throughout.

The general solutions of the scattered waves in the matrix, shell and core can be respectively expressed as

$$\begin{aligned} \varphi_s^{(1)} &= \sum_{n=0}^{\infty} A_{n1} H_n(k_{l1}r)\cos n\theta, \\ \psi_s^{(1)} &= \sum_{n=0}^{\infty} B_{n1} H_n(k_{t1}r)\sin n\theta, \end{aligned} \qquad \text{for } r \geq a, \tag{3}$$

$$\begin{aligned} \varphi_s^{(2)} &= \sum_{n=0}^{\infty} [A_{n2}J_n(k_{l2}r) + C_{n2}N_n(k_{l2}r)]\cos n\theta, \\ \psi_s^{(2)} &= \sum_{n=0}^{\infty} [B_{n2}J_n(k_{t2}r) + D_{n2}N_n(k_{t2}r)]\sin n\theta, \end{aligned} \qquad \text{for } b \leq r \leq a, \tag{4}$$

$$\begin{aligned} \varphi_s^{(3)} &= \sum_{n=0}^{\infty} A_{n3} J_n(k_{l3}r)\cos n\theta, \\ \psi_s^{(3)} &= \sum_{n=0}^{\infty} B_{n3} J_n(k_{t3}r)\sin n\theta, \end{aligned} \qquad \text{for } r \leq b, \tag{5}$$

where the superscripts 1, 2, and 3 denote the scattering fields in the matrix, shell and core, respectively, ψ is the vector potential, $N_n(\cdot)$ is the Bessel function of the second kind, $H_n(\cdot)$ the Hankel function of the first kind, k_{t1}, k_{t2}, and k_{t3} are the wave numbers of the transverse wave in the matrix, the shell, and the core, respectively, k_{l2} and k_{l3} the wave numbers of the longitudinal wave in the shell and the core, respectively. Here a and b are respectively the outer and the inner radii of the shell, A_{nm} and $B_{nm}(m = 1, 2, 3)$, and C_{n2} and D_{n2} are eight unknown coefficients.

The boundary conditions satisfied for the incident and scattered waves are continuities of the displacement and stresses on each of the two boundaries: core/shell ($r = b$) and shell/matrix ($r = a$) as follows:

$$u_{r1} = u_{r2}, \quad u_{\theta 1} = u_{\theta 2},$$
$$\sigma_{rr1} = \sigma_{rr2}, \quad \sigma_{r\theta 1} = \sigma_{r\theta 1} \quad \text{at } r = a, \tag{6}$$
$$u_{r2} = u_{r3}, \quad u_{\theta 2} = u_{\theta 3},$$
$$\sigma_{rr2} = \sigma_{rr3}, \quad \sigma_{r\theta 2} = \sigma_{r\theta 3} \quad \text{at } r = b. \tag{7}$$

Using the relations between the displacements and stresses and between the scalar and vector potentials for isotropic materials, we have

$$u_r = \frac{\partial \varphi}{\partial r} + \frac{1}{r}\frac{\partial \psi}{\partial \theta}, \tag{8}$$

$$u_\theta = \frac{1}{r}\frac{\partial \varphi}{\partial \theta} - \frac{\partial \psi}{\partial r}, \tag{9}$$

$$\sigma_{rr} = \lambda \nabla^2 \varphi + 2\mu \left[\frac{\partial^2 \varphi}{\partial r^2} + \frac{\partial}{\partial r}\left(\frac{1}{r}\frac{\partial \psi}{\partial \theta} \right) \right], \tag{10}$$

$$\sigma_{r\theta} = \mu \left[2\left(\frac{1}{r}\frac{\partial^2 \varphi}{\partial r \partial \theta} - \frac{1}{r^2}\frac{\partial \varphi}{\partial \theta} \right) + \left(\frac{1}{r}\frac{\partial \psi}{\partial r} - \frac{\partial^2 \psi}{\partial r^2} + \frac{1}{r^2}\frac{\partial^2 \psi}{\partial \theta^2} \right) \right], \tag{11}$$

where λ and μ are the Lamé constants. The eight unknown coefficients A_{nm} and $B_{nm}(m = 1, 2, 3)$, and C_{n2} and D_{n2} can be solved by the boundary conditions in Eqs.(6) and (7), and then one can obtain the wave fields in the matrix, shell and core, respectively.

If the shell material is very compliant, the oscillation of the core can be looked as that of a rigid-body and one random point of the core can be used to measure the amplitude of the core. Because the displacement is continuous at the boundary of shell/core, there must be a maximum displacement amplitude in the core at the resonant frequency whenever the local resonance occurs in the shell or in the core. Therefore one can obtain the resonant frequencies of the resonator through analysing the peaks of the core's displacement amplitude. The point of the core's center is chosen to be used for study the displacement amplitude of the core in this paper. Substituting Eq.(5) into Eqs.(8) and (9), the radial and tangential components of the core's displacement vector can be expressed as

$$u_{r3} = \sum_{n=0}^{\infty} \left[A_{n3} k_{l3} J_n'(k_{l3} r) + B_{n3} J_n(k_{t3} r)/r \right] \cos(n\theta),$$
$$u_{\theta 3} = -\sum_{n=0}^{\infty} \left[n A_{n3} J_n(k_{l3} r)/r + B_{n3} k_{t3} J_n'(k_{t3} r) \right] \sin(n\theta). \tag{12}$$

And the displacement amplitude of the core's center can be expressed in the form

$$u_{r3}|_{r=0} = \sum_{n=0}^{\infty} \left[A_{n3} k_{l3} J_n'(0) + B_{n3} k_{t3} J_n'(0) \right] \cos(n\theta),$$
$$u_{\theta 3}|_{r=0} = \sum_{n=0}^{\infty} \left[A_{n3} k_{l3} J_n'(0) + B_{n3} k_{t3} J_n'(0) \right] \sin(n\theta). \tag{13}$$

In Eq.(13), one has used the following relations:

$$\lim_{r \to 0} \frac{J_n(k_{l3} r)}{r} = k_{l3} J_n'(0),$$
$$\lim_{r \to 0} \frac{J_n(k_{t3} r)}{r} = k_{t3} J_n'(0). \tag{14}$$

Because $J_n'(\cdot) = [J_{n-1}(\cdot) - J_{n+1}(\cdot)]/2$, $J_0(0) = 1$ and $J_n(0) = 0$ for any $n \neq 0$, Eq.(13) can be expressed as

$$u_{r3}|_{r=0} = \frac{(A_{13} k_{l3} + B_{13} k_{t3})}{2} \cos(\theta),$$
$$u_{\theta 3}|_{r=0} = \frac{(A_{13} k_{l3} + B_{13} k_{t3})}{2} \sin(\theta). \tag{15}$$

Therefore the displacement amplitude of core's center can be denoted as

$$|u_3|_{r=0} = \frac{1}{2} \left| A_{13} k_{l3} + B_{13} k_{t3} \right|, \tag{16}$$

where $|u_3|_{r=0}$ is a quantitative measure of the displacement amplitude of the core's rigid-body mode.

The scattering cross section, which is defined as the total power scattered per unit length divided by the incident wave intensity (power per unit area),[14,20] can be found to be

$$Q_l = \frac{1}{k_{l1} a} \sum_{n=0}^{\infty} \varepsilon_n^{-1} \left| A_{n1} \right|^2,$$
$$Q_t = \frac{1}{k_{l1} a} \sum_{n=0}^{\infty} \varepsilon_n^{-1} \left| B_{n1} \right|^2, \tag{17}$$

where Q_l and Q_t are the non-dimensional scattering cross sections for longitudinal and transverse waves, respectively. The scattering cross sections in Eq.(17) are normalized by the constant $4a$.[20] The total scattering cross section Q_T of the layered scatter can be expressed as

$$Q_T = Q_l + Q_t. \tag{18}$$

We use the following inequalities to determine the truncation number N in the series summation in Eq.(17) of the scattering cross sections:

$$\frac{\varepsilon_{N+1}^{-1} \left| A_{(N+1)1} \right|^2}{\sum_{n=0}^{N} \varepsilon_n^{-1} \left| A_{n1} \right|^2} < 10^{-8},$$

and

$$\frac{\varepsilon_{N+1}^{-1}\left|B_{(N+1)1}\right|^2}{\sum_{n=0}^{N}\varepsilon_n^{-1}\left|B_{n1}\right|^2} < 10^{-8}. \tag{19}$$

3. The numerical results and discussion

The numerical computations are performed for a steel-silicone rubber-epoxy composite system whose physical parameters are listed in Table 1. The radius of the steel cylinder is b=5.0mm, and the thickness of silicone rubber is 2.5mm, namely a=7.5mm. The oscillation of the core can be considered as that of a rigid-body because the silicone rubber is very soft. The incident wave is a planar longitudinal wave with unit amplitude propagating along the $+x$ direction.

Table 1. The parameters of each phase in a layered cylinder, where ρ the density.

Material	Epoxy	Silicone Rubber	Steel
λ/GPa	4.43	6×10^{-4}	119.4
μ/GPa	1.59	4×10^{-5}	79.6
ρ/(kg/m^3)	1180	1300	7780

The core's displacement amplitude varying with the frequency is calculated, as shown in Fig.2, in which the frequencies related with the peaks of the core's displacement amplitude are the resonant frequencies of the layered cylinder. By studying the displacement configuration of the layered cylinder at each resonant

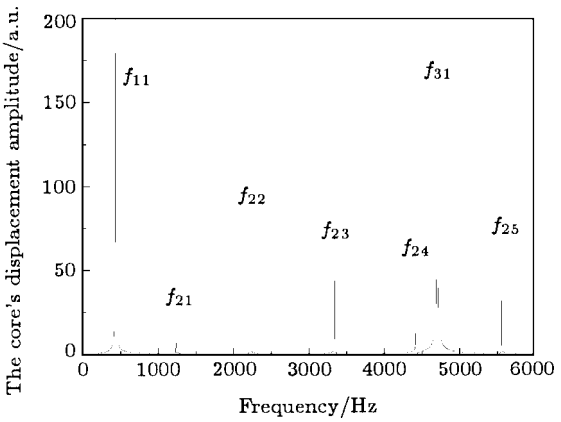


Fig.2. The core's displacement amplitude varies with the frequency. The frequencies related to the peaks are the resonant frequencies of the resonator.

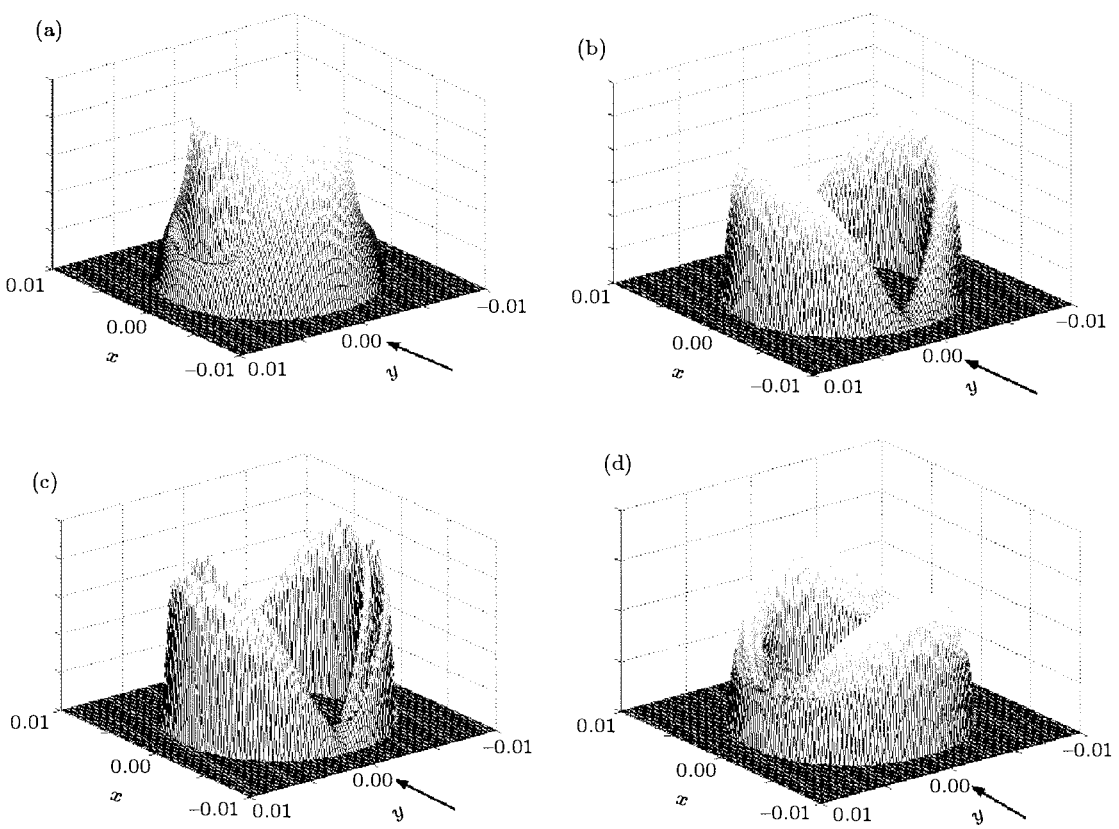


Fig.3. The displacement configurations at the resonant frequencies f_{11} (a), f_{21} (b), f_{22} (c), and f_{31} (d). The arrows indicate the direction of the incident wave.

frequency, the resonance of the single resonator can be classified typically into three kinds of the resonant modes, as shown in Fig.3. For the first kind of the resonant mode, the displacement of the core is much larger than that of the shell and also than that of matrix when the steel cylinder moves as a whole as shown in Fig.3(a). Moreover, the displacement of the shell is much larger than that of the core and also than that of the largest displacement happening in the perpendicular (parallel) incident direction for the second (third) kind of the resonant mode, as shown in Figs.3(b) and (c) (Fig.3(d)) respectively.

From Fig.2, one can find that there is only one resonant frequency for the first kind of resonant mode (represented by f_{11}), and there exist many resonant frequencies that are repeated periodically for the second and third kinds of resonant modes if we expand the range of the abscissa. In the following discussion, we represent the resonant frequency as f_{nm} (where n=2 or 3 stands for the second or third kind of resonant mode, respectively, and m refers to for the mth resonance frequency).

From Figs.3(b)–(d), one can find that standing waves are excited in the shell by the incoming wave at the second or third kind of resonant mode, and the steel cylinder remains nearly at rest compared with the rubber. One can also find that there is one anti-node for f_{21} and two anti-nodes for f_{22} in the shell; therefore, it is reasonable to conclude that there are more antinodes in the shell at higher resonant frequencies for both the second and the third kinds of resonant modes.

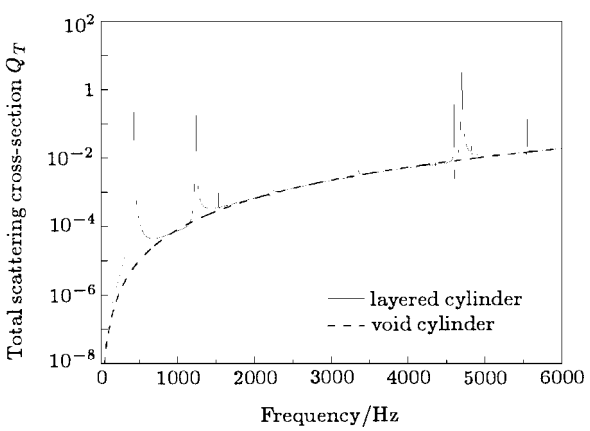


Fig.4. The total scattering cross sections of the layered cylinder and the void cylinder with a radius 7.5mm.

The total scattering cross sections of the layered cylinder and the void cylinder with a radius of 7.5mm are calculated and they have the same tendency for the variation of frequency as shown in Fig.4. By comparing Fig.4 with Fig.2, one can observe that there are strong scatterings for the layered cylinder at resonant frequencies. Therefore, the energy of the incident wave is not only absorbed by the core or shell because of resonance but also scattered out of the main path of the incident wave. The strong scattering at resonant frequencies should be also an important mechanism for the band gaps (or strong attenuation bands) of the locally resonant phononic crystal.

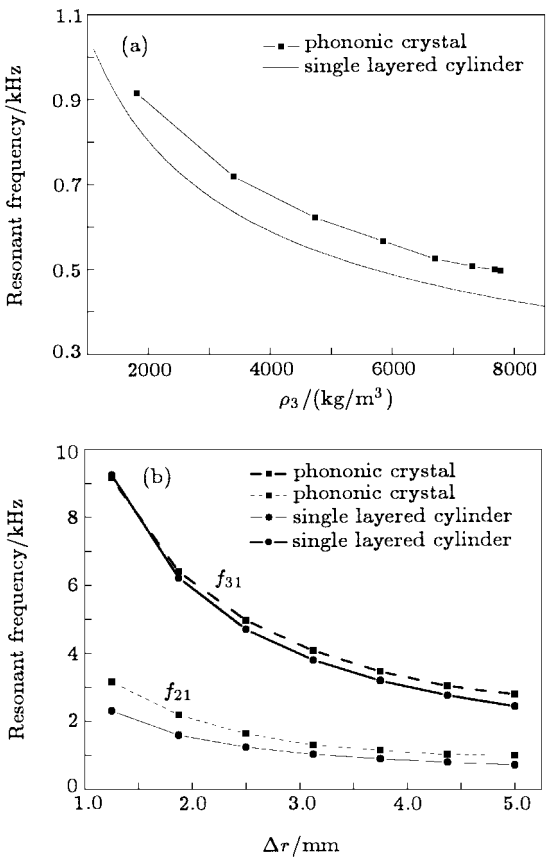


Fig.5. The f_{11} varying with the core's density (a) and the f_{21} and f_{31} varying with the shell's outer radius (b) for the single layered cylinder and the phononic crystal ($\Delta r = a - b$, b=5mm).

In order to confirm whether we can use the resonant characteristics of a single layered cylinder to evaluate the resonant characteristics of the phononic crystal, which consists of the layered cylinders, the resonant frequencies obtained from the single resonator for the parameters given in Table 1 are compared with the results of phononic crystal, calculated by LISA simulation.[13] The f_{11} varying with the core's density is compared as shown in Fig.5(a). One can see that the two curves are nearly parallel to each other and the resonant frequency of the single resonator is slightly lower than that of the phononic crystal. This shift can

be attributed to the fact that the matrix is stiffened by many layered cylinders for the phononic crystal.[24] The f_{21} and f_{31} varying with the shell's outer radius are also compared as shown in Fig.5(b), in which the slight difference can be attributed to the interaction of resonators that exists in the phononic crystal. By comparison, the three kinds of resonant modes of the single layered cylinder and those of the phononic crystal are in good agreement with each other.

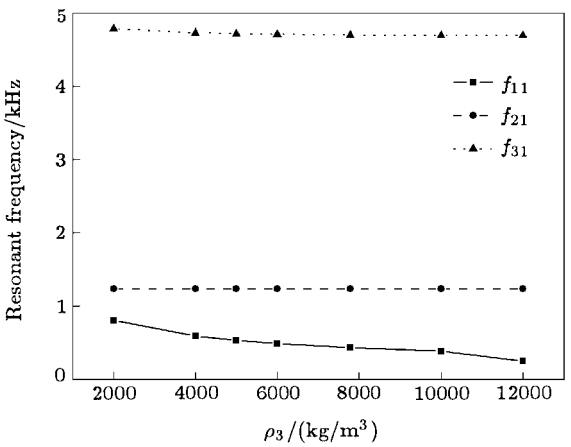


Fig.6. The f_{11}, f_{21}, and f_{31} varying with the core's density ρ_3.

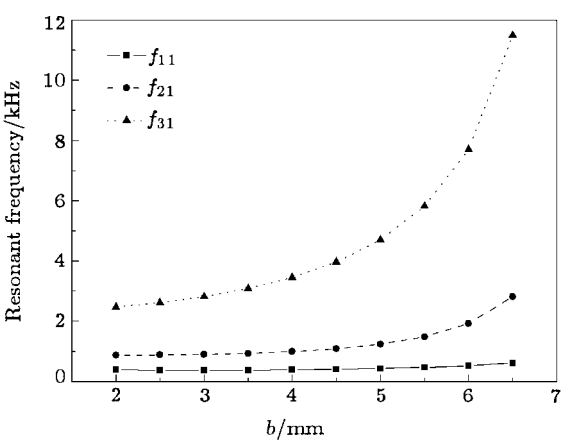


Fig.7. The f_{11}, f_{21}, and f_{31} varying with the core's radius with a=7.5mm.

The effects of the physical properties and the geometrical sizes on the resonant frequencies of each kind of resonant mode are studied, as shown in Figs.6, 7, and 8. In numerical calculations, when one parameter is taken to be varied, all other parameters remain unchanged as listed in Table 1. From Fig.6, the core's density mainly affects the f_{11}, which decreases with the increase of core's density, and the effects on the f_{21} and f_{31} can be ignored. Figure 7 shows that the f_{11}, f_{21}, and f_{31} increase with the increase of core radius; furthermore, the f_{11} increases most slowly and the f_{31} increases most quickly. Suppose that the shell material has the same Poisson ratio as the silicon rubber in Table 1: the f_{11}, f_{21}, and f_{31} varying with the shell's shear modulus μ_2 are also obtained as shown in Fig.8, in which thef_{11} increases most slowly and the f_{31} increases most quickly.

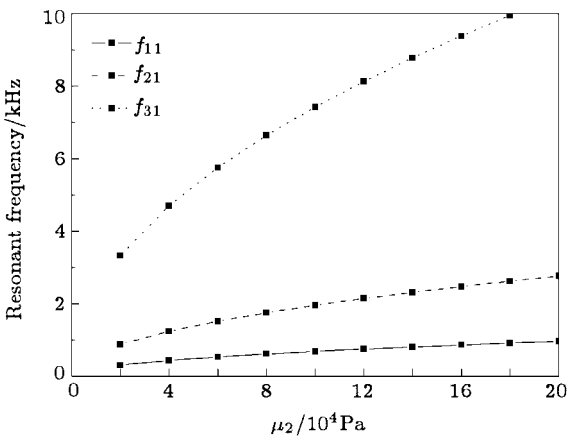


Fig.8. The f_{11}, f_{21}, and f_{31} varying with the shell's shear modulus μ_2.

4. Conclusions

In summary, the local resonant characteristics of a single layered cylinder embedded in elastic matrix is obtained through analysing the oscillation of the rigid core when the shell material is very compliant. The results show that the resonant characteristics of the phononic crystal, which consists of layered cylinders, can be evaluated by the resonant characteristics of the single layered cylinder. The strong scattering for the layered cylinder at resonant frequency is also an important mechanism for the band gaps (or the strong attenuation bands) of the phononic crystal. The effects of the geometrical and physical parameters of the layered cylinder are also studied in details. This work is significant for designing the locally resonant phononic crystal based on the local resonant characteristics of the single resonator, and the resonant frequencies can be tuned by selecting the geometrical sizes and the materials.

References

[1] Sigalas M M *et al* 1993 *Solid State Commun.* **86** 141
[2] Kushwaha M S*et al* 1994 *Phys. Rev.* B **49** 2313
[3] Montero de Espinosa F R *et al* 1998 *Phys. Rev. Lett.* **80** 1208
[4] Torres M *et al* 1999 *Phys. Rev. Lett.* **82** 3054
[5] Lambin P*et al* 2001 *Phys. Rev.* E **63** 066605
[6] Mártinez-Sala R *et al* 1995 *Nature* **378** 241
[7] Liu Z Y *et al* 2000 *Science* **289** 1734
[8] Liu Z Y *et al* 2002 *Phys. Rev.* B **65** 115116
[9] Mei J *et al* 2003 *Phys. Rev.* B **67** 245107
[10] Liu Z Y *et al* 2000 *Phys. Rev.* B **62** 2446
[11] Zhang S *et al* 2003 *Phys. Rev.* B **68** 245101
[12] Hua J, Zhang S and Cheng J C 2005 *Acta Phys. Sin.* **54** 269 (in Chinese)
[13] Hirsekorn M 2004 *Appl. Phys. Lett.* **84** 3364
[14] White R M 1958 *J. Acoust. Soc. Am.* **30** 771
[15] Jain D J *et al* 1979 *J. Appl. Phys.* **50** 4067
[16] Beattie P *et al* 1993 *J. Acoust. Soc. Am.* **94** 3421
[17] Pao Y H and Mow C C 1971 *Diffraction of Elastic Waves and Dynamic Stress Concentrations* (Crane Russack, New York) 239
[18] Sinclair A N *et al* 1993 *J. Acoust. Soc. Am.* **94** 1126
[19] Lu P and Wang Y J 2001 *Acta Phys. Sin.* **50** 697 (in Chinese)
[20] Huang W S *et al* 1995 *J. Acoust. Soc. Am.* **97** 807
[21] Yim H *et al* 1995 *Ultrasonics* **33** 377
[22] Yim H *et al* 1995 *Ultrasonics* **33** 389
[23] Cai L W 2004 *J. Acoust. Soc. Am.* **115** 515
[24] Kim J Y *et al* 1994 *J. Acoust. Soc. Am.* **95** 1213